

Realtime kinetic study of the reaction F+NO₂

D. M. Fasano and N. S. Nogar

Citation: *The Journal of Chemical Physics* **78**, 6688 (1983); doi: 10.1063/1.444668

View online: <http://dx.doi.org/10.1063/1.444668>

View Table of Contents: <http://scitation.aip.org/content/aip/journal/jcp/78/11?ver=pdfcov>

Published by the [AIP Publishing](#)



Re-register for Table of Content Alerts

Create a profile.



Sign up today!



Real-time kinetic study of the reaction $F + NO_2$

D. M. Fasano^{a)}

Department of Chemistry, University of Nebraska, Lincoln, Nebraska 68588

N. S. Nogar

Chemistry Division, MS G738, University of California, Los Alamos National Laboratory, Los Alamos, New Mexico 87545

(Received 17 December 1982; accepted 16 February 1983)

The title reaction was studied in real time by observing infrared fluorescence resulting from the competitive reaction $F + H_2$. With N_2 as a collision partner, the limiting rate constants were found to be $k_0 = 9.8 \pm 1.6 \times 10^{-31} \text{ cm}^6 \text{ molecule}^{-2} \text{ s}^{-1}$ and $k_\infty = 3.2 \pm 0.8 \times 10^{-11} \text{ cm}^3 \text{ molecule}^{-1} \text{ s}^{-1}$, as determined by fitting the experimental data to Kassel, and modified Lindemann-Hinshelwood models. Measurements with argon showed it to be slightly less effective as stabilizing the reaction complex. Calculations indicate that both FNO_2 and FONO are formed in the reaction, with a product ratio of $FONO/FNO_2 \approx 7$.

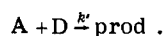
INTRODUCTION

It has been known for some time that a variety of atoms and free radicals can be produced via infrared laser induced multiphoton dissociation IRMPD.¹⁻³ More recently, species generated via IRMPD have been used in a number of chemical kinetic studies.^{3,4} One common form of study has relied on the time dependence of product vibrational (infrared) fluorescence to provide information about the reaction of interest.⁴⁻¹² The rate information usually acquired includes: the rate of disappearance of reactant atoms and the rate of relaxation of product molecules. However, two constraints typically limit the application of this technique: the exoergicity and dynamics of the reaction must produce vibrationally excited products, and the Einstein coefficient of spontaneous emission must be sufficiently large that fluorescence is competitive with collisional deactivation.

One possible method of circumventing these constraints involves the monitoring of two simultaneous reactions.^{5,12} The first reaction is a diagnostic, and must satisfy the criteria mentioned above, such that



where A is generated via IRMPD. The second reaction is unconstrained, except that it must compete with the first:



The diagnostic reaction is used to monitor the rate of disappearance of the atomic species A. The change in this rate as a function of concentration of the second reactant can then be used to determine the rate constant for the second reaction. This technique has recently been demonstrated¹² for the competitive scavenging of F atoms by CH_4 and D_2 .

In the case considered here, the reaction of interest $F + NO_2 \xrightarrow{k}$ products is studied in competition with the

diagnostic reaction $F + H_2 \rightarrow HF(\nu)$. The reaction of $F + NO_2$ is an association reaction and therefore is dependent not only on the concentration of reactants but also the bath gas. In the remainder of this paper we discuss the experimental technique, and results, including the dependence on bath gas pressure and identity. The "falloff" behavior will be compared to two proposed fitting models.¹³⁻¹⁵ Finally, possible mechanistic implications will be discussed.

EXPERIMENTAL¹⁶

The experimental technique has been described previously.^{11,12} Briefly, fluorine atoms were produced by the infrared multiphoton dissociation of SF_6 . The photolysis sources was a grating tuned CO_2 TEA laser.^{17(a)} The output was constrained to be circular by an intraactivity iris and consisted of a 45 ns spike (FWHM) containing $\approx 80\%$ of the pulse intensity, followed by a low intensity tail of 0.5 μs duration. Repetition rates were in the range of 0.5 to 0.2 Hz. Slower pulse rates were used at higher total pressures to eliminate dielectric breakdown in the focal region of the beam. Pulse energies measured with a Scientech Model 360001 were $\sim 0.8 \text{ J}$ ($\pm 5\%$) at $\gamma = 10.591 \mu\text{m}$. Wavelength determination was accomplished with an Optical Engineering CO_2 spectrum analyzer.

An Ar-coated Ge lens (focal length = 200 mm) was used to direct the beam into the photolysis cell, a stainless steel flow cell fitted with NaCl laser windows and CaF_2 viewing windows. Flow rates and pressure were controlled with micrometering valves. Infrared fluorescence was viewed at right angles to the laser beam by imaging (CaF_2 lens, focal length = 60 mm) it onto an InSb (SBRC) photovoltaic detector to 77 K. Additional fluorescence was gathered by a concave Al mirror and reflected through the cell to the detector. An interference filter (OCLI) $\lambda_{\text{max}} = 2.410 \mu\text{m}$, $\lambda_{1/2} = 2.091, 2.728 \mu\text{m}$, was used to isolate the HF fluorescence; the detector signal was coupled to a matched preamp (SBRC) and fed into a Tektronix amplifier (7A18) for further amplification. This signal was then digitized and averaged by a waveform recorder/microcomputer

^{a)}Current address: Rohm and Haas Co. Norristown and McKean Rds. Spring House, PA 19477.

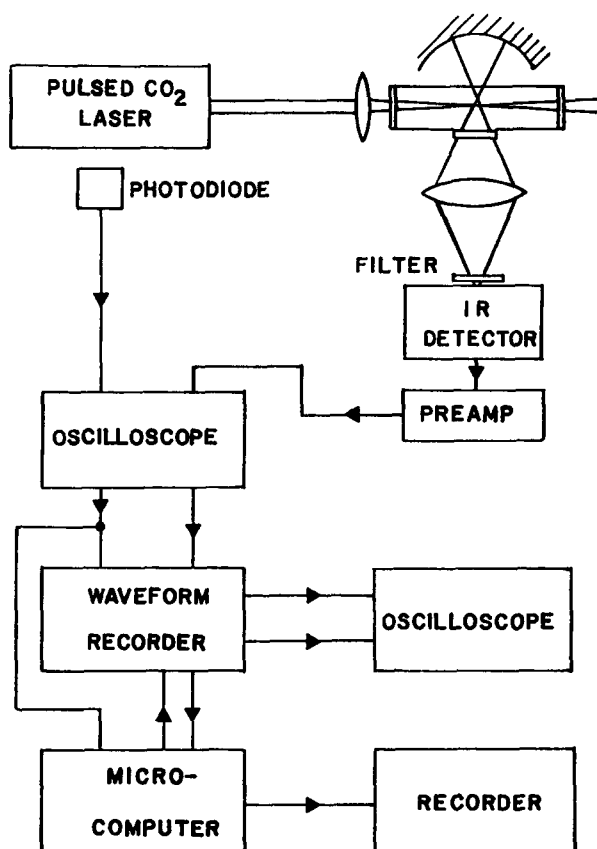


FIG. 1. Schematic of the experimental apparatus.

interface.^{17(b)} At this point the signal could be viewed on a second oscilloscope. Overall response time of the system was < 500 ns. An experimental schematic is shown in Fig. 1.

Samples were prepared by freezing SF₆ and NO₂ into an isolated cold finger of a 3 or 12 l Pyrex bulb. Hydrogen and buffer gas were then added sequentially and the warmed SF₆/NO₂ was allowed to mix. All gas handling was carried out on a glass vacuum line with base pressure $\approx 5 \times 10^{-6}$ Torr. Pressures were monitored by Validyne differential pressure transducers or a Hg manometer. Flow rates were adjusted such that the cell volume was replaced once every two seconds. With the laser pulse rates employed, this ensured that the cell volume was replaced one to five times between pulses.

The SF₆ (Scott Environmental Technology) and NO₂ (Matheson) were purified by repetitive freeze-pump-thaw cycles. The H₂, Ar, and N₂ (Matheson) were used without further purification.

RESULTS

Kinetic scheme

Fluorine atoms were generated by the infrared multiphoton decomposition of SF₆ using a pulsed CO₂ laser tuned to the P(20) line of the 00¹-10⁰ transition $\lambda = 10.591 \mu\text{m}$. This process has been well-characterized by various methods and is known to produce trans-

lationally cool F atoms by both primary and secondary processes on a time scale much faster than the subsequent reactions of interest.^{6-11,18,19} All experiments were carried out at ambient temperature 295 ± 3 K. Heating effects due to the laser have previously been shown not to be significant.⁵⁻⁷ Initial SF₆ concentrations were less than or approximately equal to the other constituents and it is estimated that < 1% dissociation of the SF₆ occurs within the focal volume of the laser.²⁰ Therefore, pseudo-first-order behavior ($[F] \ll [NO_2]$, $[M]$) is observed. No correction was necessary for the equilibrium between NO₂ and N₂O₄ as it is > 97% dissociated at all pressures used.²¹

The kinetic scheme involves the following reactions:



where the k_i are the pseudo-first-order rate constants which can be experimentally determined. The diagnostic reaction $F + H_2$ satisfies the criteria of producing a vibrationally excited product which is capable of fluorescing. In addition, this reaction has been well studied by IRMPD-infrared chemiluminescence⁷⁻¹⁰ and other techniques.²² Product energy distributions²² and the temperature-dependent thermal rates²³ are both known, so the reaction provides a well characterized diagnostic. Further, the mixture of SF₆ and H₂ with NO₂ is quite inert: no prereaction, as monitored by total pressure and infrared spectroscopy, was observed for periods of up to three days.

Reaction (3) is similarly well characterized under a variety of conditions, despite the complication¹⁰ of multiple radiative and relaxation rates from the various vibrational levels. The observed decay is thus likely to be multiexponential, dependent on the individual $k_3(\nu)$. This does not pose a serious problem as the various $k_3(\nu)$ are likely to be similar. For the case of HF, the ratio of $k_3(\nu)/k_3(1) \leq 5$ for $\nu = 2, 3$ for a variety of buffer gases.²⁴ Likewise the ratio of spontaneous emission $A(\nu - \nu - 1)/A(\nu = 1 - \nu = 0)$ is less than 2 for $\nu = 2, 3$.²⁵ Furthermore, the fraction of HF molecules which fluoresce as compared to those which collisionally deactivate is greater for $\nu = 1$ than either $\nu = 2, 3$.²⁴⁻²⁶ Therefore, in the cascading single quantum drop model of relaxation, product molecules formed in the higher vibrational levels have the greatest probability of fluorescing from the first vibrational level, regardless of the initial distribution. If a narrow bandpass filter centered about the $\nu = 1 - \nu = 0$ transition is used to observe the decay, the total pseudo-first-order decay rate will approach $k_3(\nu = 1)$. This leads to a single exponential decay with $k_3 = k_3(1)$. The set of reactions (2) and (3) thus provide a near-ideal monitor of the F-atom concentration.

The set of differential equations which describes reactions (1)–(3) can be solved exactly to yield the following expression for the time dependence of vibrationally excited product HF($\nu > 0$):

$$[\text{HF}(\nu > 0)]_t = \frac{k_2[\text{F}]_0}{k_1 + k_2 - k_3} [e^{-k_3 t} - e^{-(k_1 + k_2) t}]. \quad (4)$$

The apparent rate of HF formation (actually F-atom depletion) is given by $k_{\text{app}} = k_1 + k_2$ where $k_1 = k'_1[\text{NO}_2][\text{M}]$, $k_2 = k'_2[\text{H}_2]$, and $k_3 = k'_3[\text{M}]$ where M will include all species present and the k'_i are the appropriate ter- or bimolecular state constants. The intensity of the vibrational fluorescence $I(t)$ is proportional to the concentration of vibrationally excited HF given in Eq. (4). Deconvolution of the rising and falling portions of the signal intensity $I(t)$ will yield k_{app} and k_3 . Details of this analysis have previously been reported.^{11,12} Briefly, for all experiments $k_{\text{app}} > k_3$ so that at long times Eq. (4) reduces to

$$I(t) \propto \frac{k_2}{k_{\text{app}} - k_3} e^{-k_3 t} \quad (5)$$

and at short times the difference between Eqs. (4) and (5) yields

$$I_d(t) \propto \frac{k_3}{k_{\text{app}} - k_3} e^{-(k_{\text{app}}) t}. \quad (6)$$

A plot of the natural logarithm of Eqs. (5) and (6) yields straight lines with slopes of $-k_3$ and $-k_{\text{app}}$ respectively. A typical signal is shown in Fig. 2. The logarithmic plots are shown in Fig. 3. The good linearity of these plots supports the proposed mechanism. As a check on the consistency of these results, the parameters generated (intercept and rising and falling decay constants) were used to replicate the signal by substitution as in Eq. (4). In all cases the best-fit curve overlapped, within errors, the experimental signal. As a further test, some traces were fit via a simplex method.¹⁶ In cases where both methods were used, the same results within error limits were obtained.

As indicated previously, measurement of k_{app} as a function of NO₂ pressure allows one to determine both k_1 (from the slope of the line) and k_2 (from the intercept).

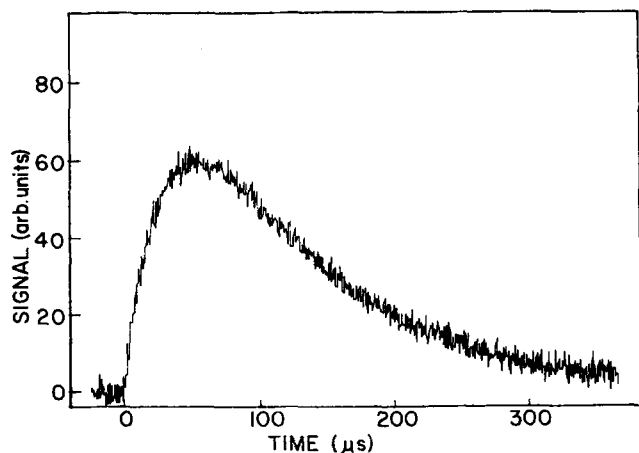


FIG. 2. Typical trace of HF fluorescence signal. Conditions of the plot include: $P_{\text{H}_2} = 20$ mT, $P_{\text{NO}_2} = 75$ mT, $P_{\text{N}_2} = 65$ T, $P_{\text{SF}_6} = 35$ mT; number of signals averaged = 256.

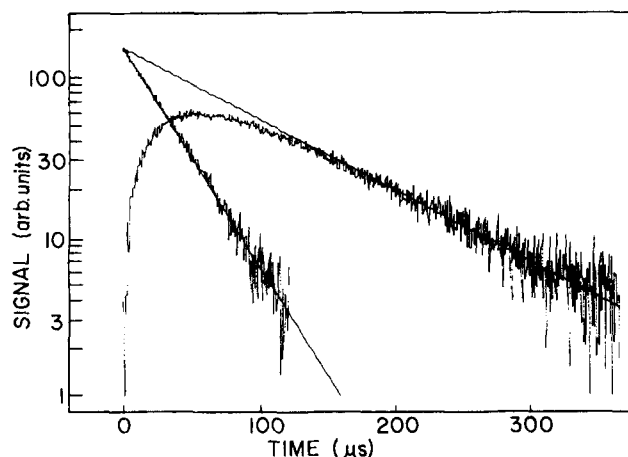


FIG. 3. Semilog plot of the data shown in Fig. 2. The linear decay portion has a slope of $k_3 = 11.2$ ms⁻¹, while the linear difference signal has a slope of $k_{\text{app}} = 31.0$ ms⁻¹.

Figure 4 shows a sample plot of k_{app} vs NO₂ concentration at an N₂ bath gas pressure of 65 Torr. Figure 5 shows the best fit lines for k_{app} vs NO₂ concentration for a variety of other N₂ and H₂ pressures. The actual data points have been eliminated for clarity. The intercepts are the rates due to the particular pressures of H₂ in each set of experiments. The fact that sets of experiments conducted at similar H₂ pressures extrapolate to approximately the same $P_{\text{NO}_2} = 0$ values lends credence to the proposed mechanism. Figure 6 shows a plot of these intercepts vs [H₂], the slope of which is k'_2 . The observed value of $2.4 \pm 0.2 \times 10^{-11}$ cm³ mol⁻¹ s⁻¹ is in excellent agreement with the rate previously reported by this method,⁶⁻¹⁰ again suggesting that the mechanism and analysis are self consistent.

The dependence of $k = k_1/[\text{NO}_2]$ concentration is shown in Fig. 7. The slight curvature is typical of the falloff region between third- and second-order kinetics. Over the range of experimental data, third-order kinetics predominates. The range of study was limited at high pressures by the onset of dielectric breakdown and the decrease of SF₆ dissociation due to pressure effects.¹⁹

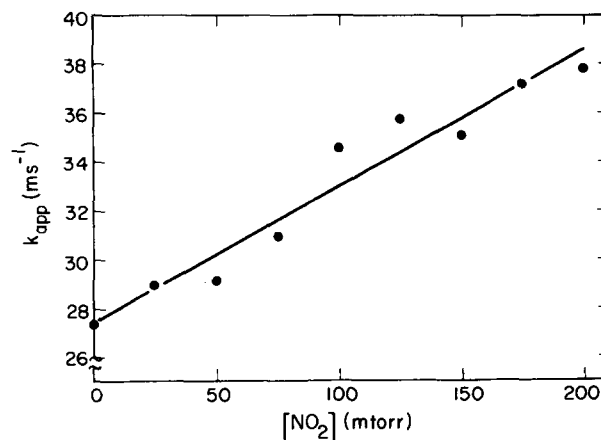


FIG. 4. A plot of k_{app} vs NO₂ at an N₂ pressure of 65 T.

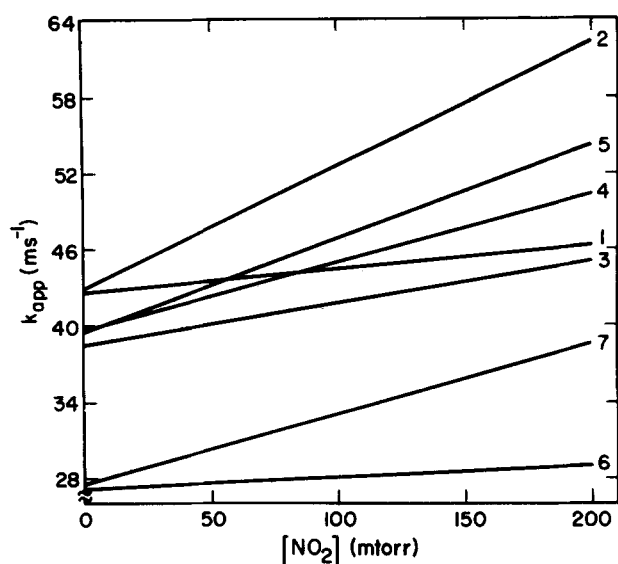


FIG. 5. The best fit lines of k_{app} vs NO_2 pressures for various N_2 and H_2 pressures; actual data points eliminated for clarity. For these curves, the experimental conditions given in the format [curve #, P_{H_2} (mTorr), P_{N_2} (Torr)] are: (1, 40, 20); (2, 40, 130); (3, 35, 30); (4, 35, 60); (5, 35, 100); (6, 20, 10); (7, 20, 65).

The low pressure limit was imposed by the difficulty in measuring the small value of the slope of k_{app} vs $[\text{NO}_2]$ at low total pressure. Higher pressure of NO_2 could not be used to increase k_{app} or it would contribute significantly to the effect of the buffer gas since it can be assumed that NO_2 is a more efficient energy transferring buffer gas than N_2 .²⁷

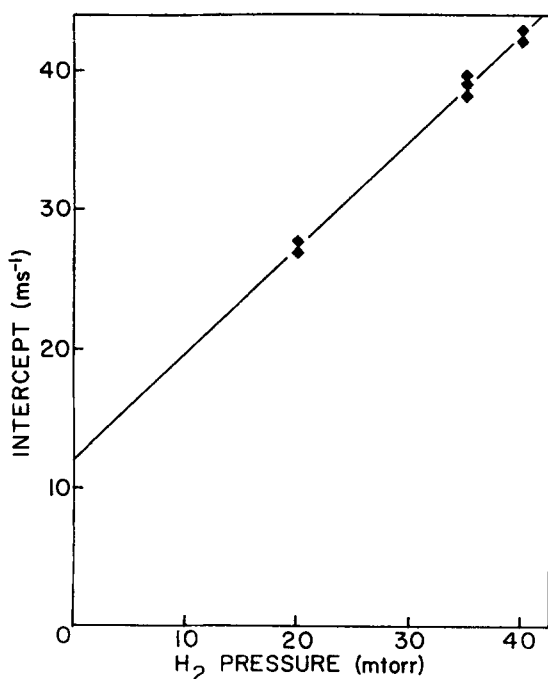


FIG. 6. Plot of intercepts from Fig. 5 as a function of H_2 pressure. The line is a linear regression fit to this data, and yields a slope of $k_2' = 2.4 \pm 0.2 \times 10^{-11} \text{ cm}^3 \text{ mol}^{-1} \text{ s}^{-1}$.

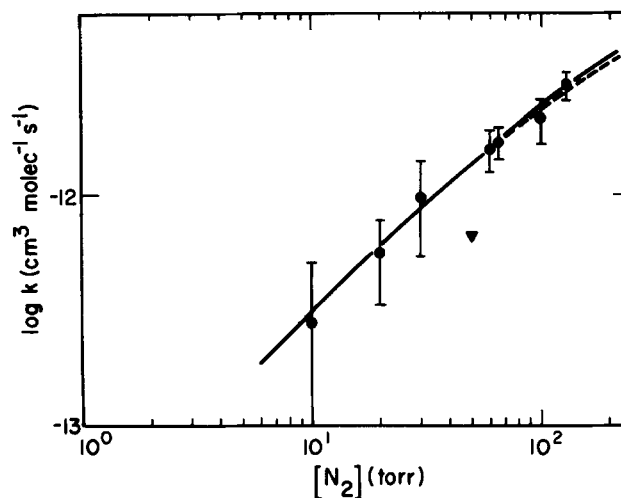


FIG. 7. The dependence of k on N_2 concentration. The lines are the best fits of the Kassel (—) and modified Lindemann-Hinshelwood (---) theories to the data. The best-fit averaged rate constants determined in this manner were $k_0 = 9.8 \pm 1.6 \times 10^{-31} \text{ cm}^3 \text{ mol}^{-2} \text{ s}^{-1}$ and $k_\infty = 3.2 \pm 0.8 \times 10^{-11} \text{ cm}^3 \text{ mol}^{-1}$. The triangle represents the Ar data.

Rate constant determination

Two methods were used to extract the limiting low and high pressure rate constants k_0 and k_∞ . Both involve fitting the data to the shape of the pressure dependence for the reverse reaction



The theory defining the pressure dependence of unimolecular dissociation is an area of extensive study. Several techniques for extracting the limiting rate constant have been devised in recent years²³ because frequently the experiment can only be performed in the falloff region where neither third- nor second-order kinetics can be isolated. Predicting the pressure dependence is simpler for reaction (7) than reaction (1) because it is dependent on the energy distribution of only one reactant. The equilibrium constant K for reactions (1) and (7) is given by $K = k_1/k_7$, is constant at a given temperature, and is independent of total pressure; therefore the pressure dependences of k_1 and k_7 are identical.

A variety of theories can be used to predict the pressure dependence of k_1 ^{14,15,28,29} and from detailed balance it follows that k_1 will have the same pressure dependence in order to maintain constant K . The pressure dependence of k_7 , and therefore k_0 and k_∞ for reaction (1), can be obtained from the data. The two models used to predict the shape of k_7 are the modified Kassel integrals¹⁴ and the Lindemann-Hinshelwood model modified for collisional energy transfer.¹⁵ We chose these simplified approaches rather than more "exact" calculations because of a lack of detailed information concerning either the nature of the transition state (*vide infra*) or the collisional stabilization process. The models used can yield good estimates of the high and low pressure limiting rate constants with even a reasonable choice of input parameters.

The Kassel integrals are dependent on two parameters S and B which are related to the number of oscillators and $E_0/k_B T$, respectively (E_0 is the threshold energy of the reaction at 0 K), and can be used to calculate the desired rate constant by

$$\frac{k}{k_\infty} = \frac{1}{\Gamma(S)} \int_0^\infty \frac{x^{S-1} e^{-x}}{1 + (k_\infty/k_0) I_0(S, B)(x/x+B)^{S-1}} dx, \quad (8)$$

where

$$I_0(S, B) = \frac{1}{\Gamma(S)} \int_0^\infty (x-B)^{S-1} e^{-x} dx. \quad (9)$$

The modification¹⁴ to the original Kassel²⁸ formulation lies in adjusting S and B to more accurately reflect the reaction and to account for the collisional efficiency of the buffer gas β_C .

Details of the calculations for this approximation are given in the Appendix. From these calculations, the reduced falloff curve can be generated.

Limiting high and low pressure rate constants for this model were obtained via a two-dimensional grid search³⁰ method by systematically varying k_0 and k_∞ . The best fit yielded

$$k_0 = 0.90 \times 10^{-30} \text{ cm}^6 \text{ mol}^{-2} \text{ s}^{-1}$$

and

$$k_\infty = 3.6 \times 15^{-11} \text{ cm}^3 \text{ mol}^{-2} \text{ s}^{-1},$$

as defined by the minimum of the sum of the residuals (the difference between the experimental and calculated values) squared.

The second method employed the Lindemann-Hinshelwood mechanism modified for collisional energy transfer. Troe and Luther¹⁵ have developed an expression to predict the shape of the falloff of k as a function of buffer gas concentration. The usefulness of this method has been shown by Zellner³¹ in expressing rates of atmospheric reactions as a function of altitude (temperature and pressure).

The expression is given below:

$$k = \frac{K_0[M]}{1 + k_0[M]/k_\infty} F_{\text{cent}} \{1 + [\log_{10}(k_0[M]/k_\infty)]^2\}^{-1}, \quad (10)$$

where the appropriate value for F_{cent} is 0.6.²³ As in the previous model k was calculated at the experimental buffer gas concentrations for systematically varied k_0 and k_∞ and the least-squares criterion was used to describe the best fit. Values obtained for the limiting rate constants were

$$k_0 = 1.06 \times 10^{-30} \text{ cm}^6 \text{ mol}^{-2} \text{ s}^{-1}$$

and

$$k_\infty = 2.8 \times 10^{-11} \text{ cm}^3 \text{ mol}^{-1} \text{ s}^{-1}.$$

We report as the best value the average of the two values with error limits equal to the range of the values

$$k_0 = 9.8 \pm 1.6 \times 10^{-31} \text{ cm}^6 \text{ mol}^{-2} \text{ s}^{-1}$$

and

$$k_\infty = 3.2 \pm 0.8 \times 10^{-11} \text{ cm}^3 \text{ mol}^{-1} \text{ s}^{-1}.$$

The experimental data and the best fit curves are shown in Fig. 7.

A set of experiments was also performed with argon as the buffer gas. The ratio of $k_{\text{Ar}}/k_{\text{N}_2}$ at 50 Torr is ~ 0.5 , which is consistent with the collision behavior of N₂ and Ar in other reactions.^{27,32} A full range study of Ar concentrations was hindered by its low collision efficiency ($\beta_{\text{Ar}} \approx \beta_{\text{N}_2}/2 \approx 0.15$) and the onset of dielectric breakdown due to the laser (< 100 Torr Ar).

The only previous data for reaction (1) employed He as the buffer gas. A value of

$$k_\infty = 6.9 \times 10^{-31} \text{ cm}^6 \text{ mol}^{-2} \text{ s}^{-1}$$

was obtained.³³ This compares favorably with previous results in which it is found that for a variety of systems^{27,32} $\beta_{\text{He}} < \beta_{\text{Ar}} < \beta_{\text{N}_2}$. The data obtained in the current work also compares favorably with the most recently recommended results²³ of

$$k_0 = 1.1 \pm 0.6 \times 10^{-30} \text{ cm}^6 \text{ mol}^{-2} \text{ s}^{-1}$$

and

$$k_\infty = 1.0 \pm 0.5 \times 10^{-10} \text{ cm}^3 \text{ mol}^{-1} \text{ s}^{-1}$$

for reaction (1) in air. The agreement for k_0 is well within the combined error limits, while for k_∞ the disagreement falls just outside the range of the combined error limits.

DISCUSSION

Throughout this study FNO₂ has been assumed as the product. It is possible, however, that the F atom could attach to either oxygen atom of NO₂ to form the isomer FONO. The existence of FONO has been postulated.³⁴ Gas phase^{35(a)} and matrix isolation^{35(b)} infrared spectra have been reported although subsequent analyses have shown the spectra to be due to the iso-electronic species HONO₂ in the case of the gas phase data and inconsistent with the proposed FONO structure in the case of the matrix isolation data.

In the analogous reaction of Cl + NO₂ a product ratio of ClONO/ClNO₂ ≤ 4 has been seen experimentally³⁶ at high pressure (700 Torr) and a ratio ≈ 5 has been obtained theoretically³⁷ for the low pressure limiting rate constant. This latter result is based on a comparison of the calculated value of $2.3 \times 10^{-31} \text{ cm}^6 \text{ mol}^{-1} \text{ s}^{-1}$ for the reaction



with the experimentally measured rate constant being $1.6 \pm 1.0 \times 10^{-30} \text{ cm}^6 \text{ mol}^{-1} \text{ s}^{-1}$.^{23,38,39} This difference is beyond the range of the respective errors (approximately a factor of 2 for the theoretical calculation) and is due to the competitive reaction to form the isomer ClONO, since the experimentally measured rate was based on the rate of disappearance of the Cl atom.

A detailed calculation of this type for the FNO₂/FONO system would not yield useful results for FONO due to the large uncertainties in assigning the necessary input

values. The only values for FONO which are available are calculated values of ΔH of isomerization for FONO \rightarrow FNO₂, and these values vary from -1.1 , -2.4 , to -25.8 kcal/mol depending on the method of calculation and the assumed molecular geometry.^{40,41} A rate constant which can be calculated is for the unimolecular dissociation reaction (7), and thus related to the association reaction by detailed balance. The necessary spectroscopic and thermodynamic data were obtained from Ref. 21 and 42, and the Lennard-Jones parameters were estimated from data for INO₂ and the XNO series: where X = F, Cl, Br, and I. A value of $k_0 = 1.2 \times 10^{-31}$ cm⁶ mol⁻¹ s⁻¹ was obtained for reaction (1) ($\beta_{cN_2} = 0.3$). Comparing this value to the experimentally derived value of $9.8 \pm 1.6 \times 10^{-31}$ indicates that the measured rate constant is a combination of more than one process. Most probably the formation of FNO₂ is in competition with the formation of FONO. The product ratio of FONO/FNO₂ is thus estimated to be 7 ± 4 . This result may change the fit to Kassel integrals, but since the shape of the falloff curve is not strongly dependent on either S_K or B_K ¹⁴ (neither of which should vary greatly for FONO) no new calculation was attempted.

CONCLUSION

A real-time competitive kinetic technique has been applied to study the reaction of atomic fluorine with nitrogen dioxide. Limiting low and high pressure rate constants were obtained by fitting the data to models of third-order reactions. Comparison with the calculated value for k_0 indicate more than a single reaction pathway exists, most probably the formation of the structural isomers FNO₂ and FONO.

APPENDIX: MODIFIED KASSEL INTEGRALS

The modified Kassel parameters S_K and B_K are obtained from the procedure outlined in Ref. 14. The necessary data is readily available or can be estimated. For reaction (7) the data is given in Table I. S_K can be obtained directly from the relation

$$S_K \cong U_{vib}/kT + 1, \quad (A1)$$

where U_{vib} is obtained from thermodynamics data ($H - H_0$), and the vibrational fundamentals ν_i .

Two intermediate parameters are then obtained, B' and S . B' is given by

$$B' = \frac{E_0 + a(E_0)E_z}{kT}, \quad (A2)$$

where E_0 is the threshold energy for the reaction, $a(E_0)$ is an anharmonicity correction, and E_z is the zero-point vibrational energy. In the case of radical species where the activation energy of the associative reaction is small

$$E_0 \cong -\Delta H_0. \quad (A3)$$

For relatively complex molecules, $a(E_0)$ is approximately unity, and

$$E_z = \frac{1}{2} \sum_{i=1}^s h\nu_i, \quad (A4)$$

where s is the number of oscillators. S is the number of effective oscillators given by

$$S = s + r/2, \quad (A5)$$

where r is the number of internal and external rotations.

$F(S, B')$ is then obtained from Table II in Ref. 14. B_K is chosen such that

$$F(S, B') = F(S_K, B_K). \quad (A6)$$

The value of S_K is affected by the collisional efficiency of the buffer gas, β_c . From Fig. 5 in Ref. 14, ΔS_K can be estimated for the previously obtained values of S_K and B_K . This value is added to S_K to obtain a new S_K . A new value of B_K is then chosen in accord with Eq. (A6). Using the values of S_K and B_K thus obtained, the reduced falloff curve can be obtained from Table I in Ref. 14.

TABLE I. Values for the determination of the modified Kassel parameters for the reaction FNO₂ + N₂ \rightarrow F + NO₂ + N₂.

Parameter	Value
ν_i	1793, 1312, 822, 742, 570 460 cm ⁻¹ ^a
ΔH_0	-52 kcal mol ⁻¹ ^a
$a(E_0)$	1
s	6
r	1
U_{vib}/kT	0.65
E_z	4.50×10^3 cm ⁻¹
E_0	1.82×10^4 cm ⁻¹
B'	110
$F(S, B')$	1.052
$F(S_K, B_K)$	
β_c	0.3
ΔS_K	0.5
S_K	$2.2 (1.65)^b$
B_K	$18 (12)^b$

^aReference 21.

^bValue in parentheses is the first approximation.

¹P. A. Schulz, Aa. S. Sudbo, A. J. Krajnovich, H. S. Kwok, Y. R. Shen, and Y. T. Lee, *Annu. Rev. Phys. Chem.* **30**, 379 (1979).

²J. L. Lyman, G. P. Quigley, and O. P. Judd, in *Multiple-Photon Excitation and Dissociation of Polyatomic Molecules*, edited by C. Cantrell (Springer, New York, 1979).

³M. N. R. Ashfold and G. Hancock, *Chem. Soc. Spec. Res. Rep.*, Vol. 4, 1980.

⁴H. Reisler, M. Mangir, and C. Wittig, in *Chemical and Biochemical Applications of Lasers*, edited by C. B. Moore (Academic, New York, 1980), Vol. 5.

⁵P. L. Houston, in *Advances in Chemical Physics*, edited by J. Jortner (Wiley, New York, 1981).

⁶(a) J. M. Presses, R. E. Weston, Jr., and G. W. Flynn, *Chem. Phys. Lett.* **48**, 425 (1977); (b) A. B. Horowitz, J. M. Presses, R. E. Weston, Jr., and G. W. Flynn, *J. Chem. Phys.* **74**, 5008 (1981).

⁷C. R. Quick and C. Wittig, *Chem. Phys. Lett.* **48**, 420 (1977).

⁸E. Wurzburg, R. J. Grimeley, and P. L. Houston, *Chem. Phys. Lett.* **57**, 373 (1978).

⁹E. Wurzburg and P. L. Houston, *J. Chem. Phys.* **72**, 4811, 5915 (1980).

- ¹⁰R. F. Heidner III, J. F. Bott, C. E. Gardner, and J. E. Melzer, *J. Chem. Phys.* **70**, 4509 (1979); **72**, 4815 (1980).
- ¹¹D. M. Fasano and N. S. Nogar, *Int. J. Chem. Kinet.* **13**, 325 (1981).
- ¹²D. M. Fasano and N. S. Nogar, *Chem. Phys. Lett.* **92**, 411 (1982).
- ¹³J. Troe, *Annu. Rev. Phys. Chem.* **29**, 223 (1978), and references therein.
- ¹⁴J. Troe, *Ber. Bunsenges Phys. Chem.* **78**, 478 (1974).
- ¹⁵J. Troe, *J. Phys. Chem.* **83**, 114 (1979); R. Luther and J. Troe, *Proceedings of the Seventeenth International Symposium on Combustion* (The Combustion Institute, Leeds, 1974).
- ¹⁶D. M. Fasano, Ph.D. dissertation, University of Nebraska, 1982.
- ¹⁷(a) W. A. Jalenak and N. S. Nogar, *Chem. Phys.* **41**, 407 (1979); *J. Phys. Chem.* **84**, 2293 (1980). (b) D. M. Fasano and N. S. Nogar, *Chem. Biomed. Environ. Inst.* **11**, 331 (1981).
- ¹⁸P. A. Schultz, Aa. S. Sudbo, E. R. Grant, Y. R. Shen, and Y. T. Lee, *J. Chem. Phys.* **72**, 4985 (1980).
- ¹⁹P. Bado and H. van den Bergh, *J. Chem. Phys.* **68**, 4188 (1978).
- ²⁰R. Duperrex and H. van den Bergh, *Chem. Phys.* **40**, 275 (1979).
- ²¹*JANAF Thermochemical Tables*, 2nd ed (Natl. Bur. Stand. U.S. G.P.O., Washington, D.C., 1971).
- ²²D. W. Setser, in *The Kinetics of Fast Reactions*, edited by I. W. M. Smith (Plenum, New York, 1980).
- ²³Jet Propulsion Laboratory Publication JPL 82-57 (1982).
- ²⁴M. A. Kwok and N. Cohen, *J. Chem. Phys.* **61**, 5221 (1974).
- ²⁵J. M. Herbelin and G. Emanuel, *J. Chem. Phys.* **60**, 689 (1974).
- ²⁶J. K. Hancock and W. H. Green, *J. Chem. Phys.* **57**, 4515 (1972).
- ²⁷(a) J. Troe, *J. Chem. Phys.* **66**, 4745, 4758 (1978). (b) D. C. Tardy and B. S. Rabinowitch, *Chem. Rev.* **77**, 369 (1977).
- ²⁸L. Kassel, *Kinetics of Homogenous Gas Reactions* (Chemical Catalog Co., New York, 1932); G. Emanuel, *Int. J. Chem. Kinet.* **4**, 591 (1972).
- ²⁹H. van den Bergh, N. Benuit Guyot, and J. Troe, *Int. J. Chem. Kinet.* **9**, 223 (1977).
- ³⁰P. A. Stark, *Introduction to Numerical Methods* (Macmillan, New York, 1970).
- ³¹R. Zellner, *Ber. Bunsenges. Phys. Chem.* **82**, 1172 (1978).
- ³²N. S. Nogar and L. D. Spicer, *J. Chem. Phys.* **66**, 3624 (1977).
- ³³C. Fetzsch, *Combustion Institute European Symposium* (Academic, London, 1973).
- ³⁴R. D. Sprately and G. C. Pimentel, *J. Am. Chem. Soc.* **88**, 2384 (1966).
- ³⁵(a) P. J. Brune, J. E. Sicre, and H. J. Schumacher, *Chem. Commun.* **241**, (1970); J. E. Sicre and H. J. Schumacher, *Z. Anorg. Allg. Chem.* **385**, 131 (1971). (b) R. R. Smardzewski and W. B. Fox, *Chem. Commun.* **241**, (1974); *J. Am. Chem. Soc.* **96**, 304 (1974).
- ³⁶H. Niki, P. D. Maker, C. M. Savage, and L. P. Breitenbach, *Chem. Phys. Lett.* **59**, 78 (1978).
- ³⁷J. S. Chang, A. C. Baldwin, and D. M. Golden, *J. Chem. Phys.* **71**, 2021 (1979).
- ³⁸A. R. Ravishankara, G. Smith, and D. D. Davis, Talk presented at the Thirteenth Informal Photochemistry Conference, Clearwater Beach, Florida, 1978.
- ³⁹M. S. Zahniser, J. S. Chang, and F. Kaufman, *J. Chem. Phys.* **67**, 997 (1977).
- ⁴⁰P. S. Ganguli and H. A. McGee, Jr., *Inorg. Chem.* **11**, 3071 (1972).
- ⁴¹M. J. S. Dewar and H. S. Rozepa, *J. Am. Chem. Soc.* **100**, 58 (1978).
- ⁴²J. O. Hirschfelder, C. F. Curtiss, and R. B. Bird, *Molecular Theory of Gases and Liquids* (Wiley, New York, 1963).